Static and dynamic characteristics of magnetized journal bearings lubricated with ferrofluid

T.A. Osman [a,*], G.S. Nada [b], Z.S. Safar [b]

[a] *Department of Mechanical Design and Production, Faculty of Engineering, Cairo University, Cairo, Egypt*
[b] *Department of Mechanical Power, Faculty of Engineering, Cairo University, Cairo, Egypt*

Abstract

This work was concerned with the static and dynamic characteristics of the hydrodynamic journal bearings lubricated with ferrofluid. Based on the momentum and continuity equations, a pressure differential equation (modified Reynolds equation) was obtained. Assuming linear behavior for the magnetic material of the ferrofluid, the magnetic force was calculated. The magnetic pressure resulting from the magnetic force was incorporated into the Reynolds equation and it was not separately treated. The equation was solved numerically by the finite difference procedure, obtaining the appropriate iterative technique and pressure distributions. The load-carrying active region and cavitation region boundary shapes could be then determined. The solution renders the bearing performance characteristics, namely, load carrying capacity, attitude angle, frictional force at the journal surface, friction coefficient and bearing side leakage. By the finite perturbation technique, the eight-oil film stiffness and damping coefficients were determined. The dynamic coefficients were used as input data for studying the stability characteristics of the rotor-bearing system. The critical speed at which whirling motion begins to occur was calculated. © 2001 Elsevier Science Ltd. All rights reserved.

1. Introduction

Ferrofluids consist of three basic components, namely, a base fluid or carrier fluid, ferromagnetic particles and a coating on each particle [1]. Ferrofluids are an interesting group of liquids, because they have liquid properties and act like a ferromagnetic material. Many properties of the ferrofluid are similar to those of the base fluid. Since the concentration of the magnetic particles is low, 3–10%, they do not affect the density, vapor pressure, pour point, or chemical properties of the liquid, but there is an increase of the ferrofluid viscosity compared with the viscosity of its base fluid [2]. Ferrofluid properties were studied by Rosensweig [2,3], Miyake and Takahashi [4], and Goldowsky [5].

Ferrofluids can solve many difficult sealing, lubricating, detection, heat transfer and damping problems. Applications of ferrofluids are usually based on their controllability by an external magnetic force [6]. Ferro-

fluids and devices incorporating them have found applications in high-vacuum equipment, laser systems, computers, inertia dampers, loudspeakers, material separation, domain detection and many other areas. Among the various applications in engineering are those taking advantage of the possibility of collecting and holding firmly small quantities of such fluids in a region with highly focused magnetic fields. From this viewpoint, ferrofluids were derived to be used in liquid seals [7,8] and hydrodynamic braking systems [9]. The most recent application is in the MagneRide, a damping suspension system developed by Delphi Automotive [10]. It is a fully integrated algorithmic control. According to Delphi engineers, the applications of magneto-rheological fluids enable instantaneous responses, high performance levels, virtually silent operation, and the elimination of electromechanical valves. Delphi expects the first MagneRide systems to appear on passenger vehicles in 2003.

Only a few and incidental references have been made to the field of lubrication. Analytical investigations have already been executed [10–12] and the theoretical results

---

* Corresponding author. Tel.: +20-2567-8151; fax: +20-1133-4504.

Nomenclature

c	bearing clearance
D	bearing diameter
F_j	friction force at the journal surface
h	lubricant film thickness
H	dimensionless film thickness, $H=h/c$
h_m	magnetic field intensity
H_m	dimensionless magnetic field intensity, $H_m=h_m/h_{mo}$
L	bearing length
m	half mass of the rotor
M_g	magnetization of the ferrofluid
M	dimensionless mass of the rotor-bearing system, $M=\omega^2 cm/w$
M_{cr}	critical value of M
p	lubricant pressure
P	dimensionless pressure, $P=[p(c/R)^2]/\eta\omega$
q	bearing side leakage
Q	dimensionless side leakage, $Q=2q/LRc\omega$
R	bearing or journal radius
t	time
v_x	circumferential velocity component
v_y	radial velocity component
v_z	axial velocity component
v_s	squeeze velocity of the journal center
w	load carrying capacity
w_x	load component in vertical direction
w_y	load component in horizontal direction
W	dimensionless load carrying capacity, $W=[w(c/R)^2]/\eta\omega LR$
W_ε	dimensionless load capacity component in the eccentricity direction
W_ϕ	dimensionless load capacity component in the direction normal to the eccentricity
X_m	susceptibility of ferrofluid
x, y, z	cartesian coordinates
Z	dimensionless axial distance, $Z=z/L$
ε	eccentricity ratio
η	fluid viscosity
θ	angular coordinate $\theta=x/R$
μ_o	permeability of free space or air $\mu_o=4\pi\times10^{-7}$ AT/m
τ	dimensionless time
ω	angular speed
ω_{cr}	critical rotor speed

are restricted to only two classical limiting cases of infinitely long and short bearings. Sorge [14] in his numerical approach to finite journal bearings assumed the distribution of the pressure to be caused by the magnetic field. This assumption is far from correct. The magnetic force must be calculated firstly from the assumed magnetic field distribution model and then substituted into the equations of motion of the fluid film. These works and another [14] were interested in the static characteristics of these magnetized journal bearings; none of them determined the dynamic characteristics. This work is the first attempt at studying the dynamic behavior of journal bearings lubricated with ferrofluid. Overall, character-

istics including pressure distributions, cavitation region boundary shape, load carrying capacity, attitude angle, friction, side leakage, stiffness and damping coefficients will be determined. In addition, the stability characteristics of a system composed of a rotor supported on two identical bearings are calculated.

It must be noted that the most important property of the ferrofluid is its magnetization. Usually it is a function of temperature and applied magnetic field. If temperature variation is small, the magnetization can be regarded as independent of temperature. Thus the magnetization is only dependent on the applied field. The property of the magnetization under this condition can be roughly div-

ided into two parts. If an applied field is strong enough, the magnetization of the fluid reaches a saturation state and is almost constant. On the other hand, if an applied field is small, the magnetization of the fluid is approximately proportional to the applied field. The objective of this paper is to determine the overall static and dynamic characteristics of the finite hydrodynamic journal bearing lubricated with ferrofluid under an applied axial symmetric field. Evaluation of the ferrofluid, under this field distribution, as a lubricant can then be verified. Tipei [11] supposed that the field may be represented by parabolic distribution in the axial direction. This distribution was also assumed by Chang et al. [17] in their theoretical and experimental study of a ferrofluid lubricated four-pocket journal bearing. In their work, reasonable agreement was obtained between the theoretical and experimental results, in which a permanent magnet was used as the magnetic field source. This model still needs further analysis for studying the influence of its parameters on the overall characteristics of the bearing.

2. Modified Reynolds equation

For a ferrofluid under a magnetic field, the unit volume value of the induced magnetic force is given by $f_m=(\mathrm{curl}\ h_m)B+\mu_o M_g\cdot\mathrm{grad}\ h_m$ [15,16], where B is the magnetic field density and curl h_m represents the induced free current. For non-conductive base fluid, no free currents are induced. Considering isothermal conditions and linear behavior of the ferrofluid, $M_g=X_m h_m$, the induced magnetic force can be given as:

$$f_m=\mu_o X_m h_m \mathrm{grad}\ h_m \tag{1}$$

Starting from the basic Navier–Stokes equations and using the magnetic force as a body external force, the equations of motion for the fluid film are derived as follow.

$$0=-\frac{\partial p}{\partial x}+\eta\frac{\partial^2 v_x}{\partial^2}+f_{mx} \tag{2}$$

$$0=-\frac{\partial p}{\partial z}+\eta\frac{\partial^2 v_z}{\partial^2}+f_{mz} \tag{3}$$

where f_{mx} and f_{mz} are the magnetic force components in the circumferential and axial directions, respectively. For axial symmetric applied field $\partial h_m/\partial x=0$ and Eq. (1) gives $f_{mx}=0$. Integrating Eqs. (2) and (3) twice and using the boundary conditions, $v_x(h)=\omega R$, $v_y(h)=v_s$, $v_z(h)=0$ and $v_x(0)=v_y(0)=v_z(0)=0$, velocity profiles in the circumferential and axial directions are obtained.

$$v_x=\frac{1}{2\eta}\frac{\partial p}{\partial x}(y^2-yh)+\omega R\frac{y}{h} \tag{4}$$

$$v_z=\frac{1}{2\eta}\frac{\partial p}{\partial z}(y^2-yh)-\frac{1}{2\eta}f_{mz}(y^2-yh) \tag{5}$$

Substituting these velocity distributions into the integrated continuity equation, a non-dimensional modified Reynolds equation is obtained in the form:

$$\frac{\partial}{\partial\theta}\left(H^3\frac{\partial P}{\partial\theta}\right)+\frac{1}{4v^2}\frac{\partial}{\partial Z}\left(H^3\frac{\partial P}{\partial Z}\right)=6\frac{\partial H}{\partial\theta}+12(\varepsilon\cdot\cos\theta$$
$$+\varepsilon\phi\cdot\sin\theta)+\alpha\frac{\partial}{\partial Z}\left(H^3 H_m\frac{\partial H_m}{\partial Z}\right) \tag{6}$$

For this equation, the magnetic effect cannot be separately treated and superimposed onto the hydrodynamic effect as in [10,11,13] since the pressure boundary is not fixed. In journal bearing lubrication, there is a free boundary condition and the cavitation region is affected by the pressure itself.

3. Bearing scheme

The examined journal bearing is schematized in Fig. 1. It is an axial feeding cylindrical finite journal bearing. The geometric axes of the journal and bearing are assumed parallel. Then, the non-dimensional film thickness is given by:

$$H=1+\varepsilon\cos\theta \tag{7}$$

Considering the boundary conditions, it is clear that the hydrodynamic pressure and the magnetic force are symmetrical about the middle plane of the bearing ($Z=0$). Thus only half of the bearing has to be calculated. The boundary conditions used are:

$$\frac{\partial P}{\partial Z}(\theta,0.0)=0,\ P(0.0,Z)=P(2\pi,Z)=0,\ P(\theta,0.5)=0 \tag{8}$$

At film rupture and reformation boundaries, free Reynolds boundary conditions are used:

$$P(\theta^*)=\frac{\partial P}{\partial\theta}=0.0 \tag{9}$$

θ^* is the film rupture or reformation angle; it is not a prescribed value but it is determined during calculations. Two bearing configurations are used. The first is simple, Fig. 1(a). The other is equipped with ferrofluid seals, Fig. 1(b). There is no difference in boundary conditions for the two configurations. The seals' size is very large compared with the bearing clearance such that the pressure inside them (atmospheric pressure) is not affected by shaft rotation. In this case the fluid seal works as a sink (for the active positive-pressure regions) where the lubricant flows from the gap high-pressure regions to the seal. It works as a source (for the cavitation region) where the lubricant flows from the seal to the gap zero-pressure regions by the effect of the axial magnetic force f_{mz}. The effect of the two side seals on the side leakage will be determined.
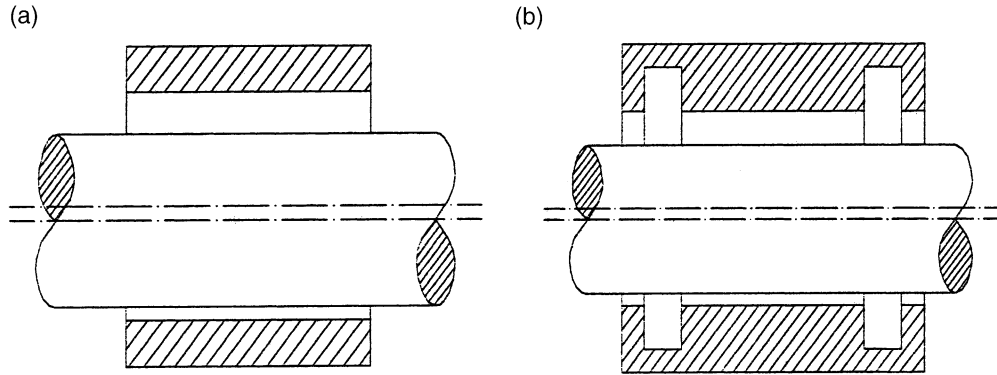
Fig. 1. Schematic diagram of bearing configuration. (a) Conventional bearing, and (b) sealed bearing.

4. Magnetic field model

The axial parabolic distribution magnetic field is used. It is represented by the following equation:

$$h_m(z) = h_{mc} - (h_{mc} - h_{me})(2z/L)^2 \tag{10}$$

In non-dimensional form, it is given by:

$$H_m(z) = 1.0 - 4(1 - \beta)Z^2 \tag{11}$$

where $H_m = h_m/h_{mc}$ and $Z = z/L$.

β is the ratio of the magnetic field strength at the end section (h_{me}) to its value at the middle section (h_{mc}). It is an important parameter that determines the gradient of the magnetic field. Negative magnetic gradient is required to obtain positive induced magnetic pressures and the resultant load carrying capacity will then be increased. This can be achieved for values of β ranging from 0.0 to less than 1.0. If $\beta = 1.0$, there is no field variation ($\partial H_m/\partial Z = 0.0$) and Eq. (6) will be turned into the classical Reynolds equation for the hydrodynamic lubrication and the bearing will then perform as a conventional bearing. On the other hand, if the magnetic field variation is such that $\partial H_m/\partial Z$ is positive (for $\beta > 1.0$), negative magnetic pressures will be induced and the bearing performance is then decreased.

To examine the effect of magnetic parameter (β), the magnetic term in the modified Reynolds equation $\partial/\partial Z[H_m(\partial H_m/\partial Z)]$ is plotted against the axial bearing distance (Z) for different values of β, Fig. 2. As shown, for $\beta = 1.0$, the magnetic term has zero value and no gain is obtained. For $\beta = 0.75$, it is clear that the magnetic term is negative along the whole bearing. The results of the positive induced magnetic pressures and the bearing characteristics are then improved. For $\beta = 0.5$, there is an increase in the negative values of the magnetic term at the bearing central region with a small region of positive values near the bearing end. With further decreases in β, the negative values in the central region are further increased but with extension of the positive values region to the inside of the bearing. This will add positive pressure at the bearing central region and negative press-
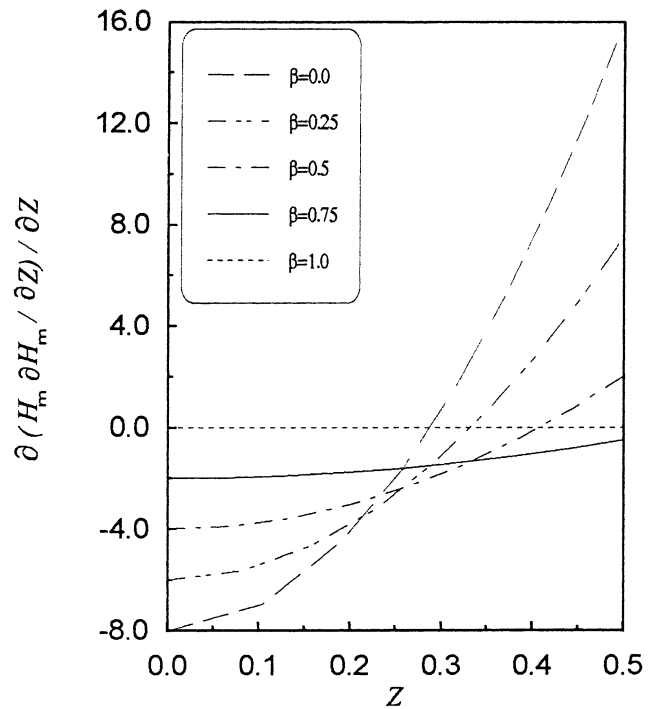

Fig. 2. Influence of parameter (β) on the magnetic term $\partial(H_m\partial H_m/\partial Z)\partial Z$.

ure near the bearing ends. Fig. 3 shows the effect of magnetic parameter (β) on the sealing magnetic force term $[H_m(\partial H_m/\partial Z)]$ at the bearing end. It shows that the maximum sealing effect is obtained for $\beta = 0.5$.

Another important parameter that determines the strength of the magnetic effect is the magnetic force coefficient $\alpha = [(h_{mo})^2\mu_o X_m c^2]/\eta\omega L^2$. Its value is determined as follows. In this work, the ferrofluid is studied in its linear behavior range, so the magnetic field must not exceed a certain limited value above which the magnetization of the ferrofluid becomes constant and saturated. The characteristic value (h_{mo}) for this model equals h_{mc} (the magnetic field strength at the bearing central section). For $h_{mc} = 10^3$ A/m and supposing $X_m = 2.0$, the magnetic force coefficient corresponding to
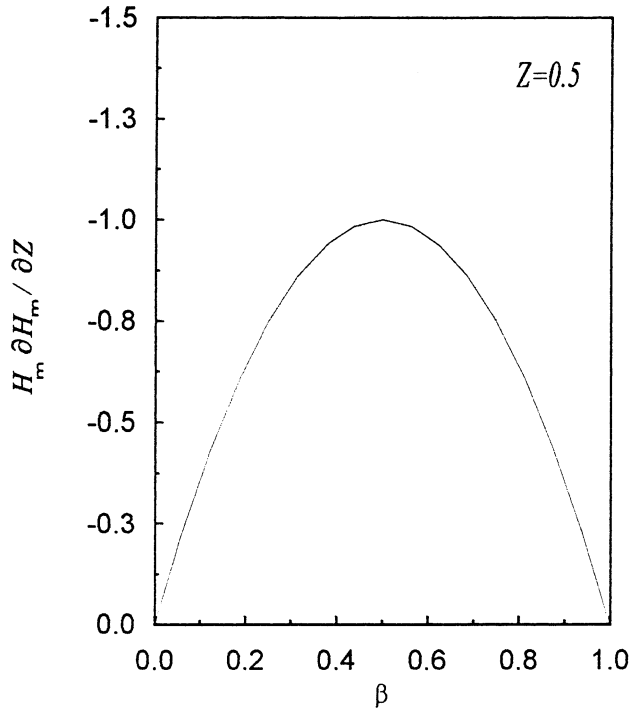
Fig. 3. Influence of parameter (β) on the sealing magnetic force term $H_m \partial H_m / \partial Z$.

loose and low speed bearings can be estimated using $\eta = 10^{-4}$ kg/m s (glycerol lubricant which most often is the carrier in ferromagnetic suspensions [12]), $c/L = 10^{-2}$ and $\omega = 10$ s^{-1}. According to the above-assumed values, the magnetic force coefficient is equal to $\alpha \cong 0.25$. Three different values starting from $\alpha = 0.05$ (accounting for increases in speed and small clearances), 0.1 and 0.2 are used. This leads us to fully analyze the effect of α and understanding completely the mechanism by which the bearing performance is modified with the magnetic lubrication.

5. Static characteristics

The bearing static characteristics are firstly calculated by making the squeeze film action term ($\varepsilon \cos \theta + \varepsilon \phi \sin \theta$) equal to zero. Then Eq. (6) can be solved numerically by the finite difference technique and pressure distributions are obtained. The extent of the active pressurized region (positive pressure region) and cavitation region (zero-pressure region) boundaries, thus, can be determined. Integration of the pressure over the bearing area gives the non-dimensional load carrying capacity, calculated by:

$$W = \sqrt{W_\varepsilon^2 + W_\phi^2}$$

$$W_\varepsilon = 2 \int_0^{0.5} \int_0^{2\pi} P \cos \theta \, d\theta \, dZ \tag{12}$$

$$W_\phi = 2 \int_0^{0.5} \int_0^{2\pi} P \sin \theta \, d\theta \, dZ$$

The Sommerfeld number, S, can be determined as:

$$S = \frac{1}{\pi W} \tag{13}$$

The attitude angle, ϕ, is calculated by:

$$\phi = \tan^{-1} \left(\frac{-W_\phi}{W_\varepsilon} \right) \tag{14}$$

Non-dimensional frictional force at the journal surface can be given by:

$$F = 2 \int_0^{0.5} \int_0^{2\pi} \left(0.5 \frac{\partial P}{\partial \theta} H + \frac{\bar{k}}{H} \right) d\theta \, dZ \tag{15}$$

where $F = [(c/R)^2 / \eta \omega L c] F_j$ and $\bar{k}$ is a control number. Inside the active zone region (full film thickness), $\bar{k} = 1.0$ and outside this region (partial film thickness), it is calculated by $\bar{k} = h_{min}/h < 1.0$; where h_{min} is the minimum film thickness.

The side leakage can be obtained by integrating the axial velocity component v_z across the end section. In general, it is calculated by:

$$Q = \int_0^{2\pi} -\frac{H^3}{6} \left(\frac{1}{4v^2} \frac{\partial P}{\partial Z} - \alpha H_m \frac{\partial H_m}{\partial z} \right)_{z=0.5} d\theta \tag{16}$$

6. Dynamic characteristics

Since in journal bearings the directions of external load and corresponding movement of journal center do not generally coincide, the state of equilibrium of a rotating shaft supported by journal bearings becomes unstable under certain conditions. When the journal vibrates, squeeze film pressure is also generated in addition to the wedge film pressure. These pressures give rise to spring and damping forces of the oil film and therefore influence the stability of the rotor-bearing system. Considering the coordinate system shown in Fig. 4, the components of the oil film force can be written as:

$$w_x = w_x(x, y, \dot{x}, \dot{y}), \quad w_y = w_y(x, y, \dot{x}, \dot{y}) \tag{17}$$

These non-linear functions can be expressed as a linear function, for small amplitude of vibration, of the displacement and velocity of the journal center by using a first-order Taylor series expansion. The force system has the following form:
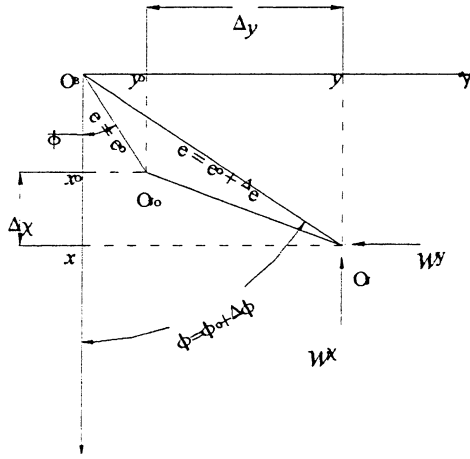
Fig. 4.   Small vibration in the vicinity of the static equilibrium point.

$$w_x = w_{xo} + \left(\frac{\partial w_x}{\partial x}\right)_o \Delta x + \left(\frac{\partial w_x}{\partial y}\right)_o \Delta y + \left(\frac{\partial w_x}{\partial \dot{x}}\right)_o \Delta \dot{x} + \left(\frac{\partial w_x}{\partial \dot{y}}\right)_o \Delta \dot{y}$$

$$w_y = w_{yo} + \left(\frac{\partial w_y}{\partial x}\right)_o \Delta x + \left(\frac{\partial w_y}{\partial y}\right)_o \Delta y + \left(\frac{\partial w_y}{\partial \dot{x}}\right)_o \Delta \dot{x} + \left(\frac{\partial w_y}{\partial \dot{y}}\right)_o \Delta \dot{y}$$

(18)

where subscript (o) denotes that the load components and partial derivatives are evaluated at the equilibrium position. The linear stiffness and damping coefficients are then defined as:

$$k_{xx} = \left(\frac{\partial w_x}{\partial x}\right)_o, \; k_{xy} = \left(\frac{\partial w_x}{\partial y}\right)_o, \; k_{yx} = \left(\frac{\partial w_y}{\partial x}\right)_o, \; k_{yy} = \left(\frac{\partial w_y}{\partial y}\right)_o$$

$$c_{xx} = \left(\frac{\partial w_x}{\partial \dot{x}}\right)_o, \; c_{xy} = \left(\frac{\partial w_x}{\partial \dot{y}}\right)_o, \; c_{yx} = \left(\frac{\partial w_y}{\partial \dot{x}}\right)_o, \; c_{yy} = \left(\frac{\partial w_y}{\partial \dot{y}}\right)_o$$

The non-dimensional form of stiffness and damping coefficients is given by:

$$\bar{K}_{ij} = k_{ij} \frac{c}{w} \qquad \bar{C}_{ij} = c_{ij} \frac{c\omega}{w}$$

(19)

$\bar{K}_{ij}$ and $\bar{C}_{ij}$ can be determined when the partial derivatives at the static equilibrium point are given. Small perturbations will be given from the static equilibrium position with respect to ε, ϕ, $\dot{\varepsilon}$ and $\dot{\phi}$, respectively and substituting into the Reynolds Eq. (6). Small variations in the film reaction force will be obtained. Due to the non-linear nature of the oil film forces, the calculated results by this finite perturbation method are sensitive to the amplitude of perturbation when the amount of perturbation is large. If the perturbation amplitude is about (or less than) 10^{-2}, the obtained partial derivatives are constant (independent of perturbation amplitude) and agree with those obtained by the zero-amplitude perturbation method [18,19]. Another non-dimensional form of the stiffness and damping coefficients is convenient to use and has the following form:

$$K_{ij} = \frac{\bar{K}_{ij}}{S} = k_{ij} \frac{c}{Sw} = k_{ij} \frac{\pi(c/R)^3}{\eta \bar{\omega} L}$$

(20)

$$C_{ij} = \frac{\bar{C}_{ij}}{S} = c_{ij} \frac{c}{Sw} = c_{ij} \frac{\pi(c/R)^3}{\eta L}$$

According to this non-dimensional form, the stiffness and damping coefficients only depend on the bearing geometrical parameters.

The effect of ferrofluid lubrication on the dynamic coefficients will be reflected on the stability of the rotor-bearing system. In this analysis the bearing stability is determined by the onset of whirl instability for a rigid rotor supported by two identical journal bearings. For this system, considering the coordinates shown in Fig. 4, the equations of motion linearized about the equilibrium position can be written in non-dimensional form as:

$$M\ddot{X} + \bar{C}_{xx}\dot{X} + \bar{C}_{xy}\dot{Y} + \bar{K}_{xx}X + \bar{K}_{xy}Y = 0.0$$

(21)

$$M\ddot{Y} + \bar{C}_{yy}\dot{Y} + \bar{C}_{yx}\dot{X} + \bar{K}_{yy}Y + \bar{K}_{yx}X = 0.0$$

where $X = x/c$, $Y = y/c$, $\dot{X} = \mathrm{d}X/d\tau$, $\ddot{X} = \mathrm{d}^2X/d\tau^2$, $t = \omega\tau$, $\bar{K}_{ij} = k_{ij}(c/w)$, $\bar{C}_{ij} = c_{ij}(c\bar{\omega}/w)$, w is the force on each bearing $= mg$ (for a horizontal rotor), $M = (\bar{\omega}^2 cm)/w$ is the non-dimensional mass of the system, and its square root $\omega\sqrt{cm/w}$ is the non-dimensional speed of the rotor.

According to the work of Lund [19], the threshold of stability is given by:

$$M_{cr} = \frac{\bar{\omega}_{cr}^2 mc}{w} = \frac{\bar{K}_o(\bar{C}_{yy}\bar{C}_{xx} - \bar{C}_{xy}\bar{C}_{yx})}{(\bar{K}_{xx} - \bar{K}_o)(\bar{K}_{yy} - \bar{K}_o) - \bar{K}_{xy}\bar{K}_{yx}}$$

(22)

where

$$\bar{K}_o = \frac{\bar{K}_{xx}\bar{C}_{yy} + \bar{K}_{yy}\bar{C}_{xx} - \bar{K}_{xy}\bar{C}_{yx} - \bar{K}_{yx}\bar{C}_{xy}}{\bar{C}_{yy} + \bar{C}_{xx}}$$

The non-dimensional critical speed of the rotor is then given by:

$$\bar{\omega} = \omega_{cr}\sqrt{\frac{mc}{w}} = \sqrt{M_{cr}} = \sqrt{\frac{\bar{K}_o(\bar{C}_{xx}\bar{C}_{yy} - \bar{C}_{xy}\bar{C}_{yx})}{(\bar{K}_{xx} - \bar{K}_o)(\bar{K}_{yy} - \bar{K}_o) - \bar{K}_{xy}\bar{K}_{yx}}}$$

(23)

This critical speed will be used for expressing the threshold stability of the rotor-bearing system.

7. Results and discussion

The performance characteristics of a magnetized bearing, with length to diameter ratio $\nu = 1.0$ and magnetic parameter $\beta = 0.75$, are determined and compared to those of a conventional lubricated bearing, i.e. a bearing which has zero magnetic force coefficient α.

Fig. 5 shows the centerline pressure distributions for different magnetic force coefficients α and $\varepsilon = 0.1$. It is clearly shown that, there is a considerable increase in pressure through the whole section. This increase is due to the negative gradient of the magnetic field $(\partial H_m/\partial Z)$
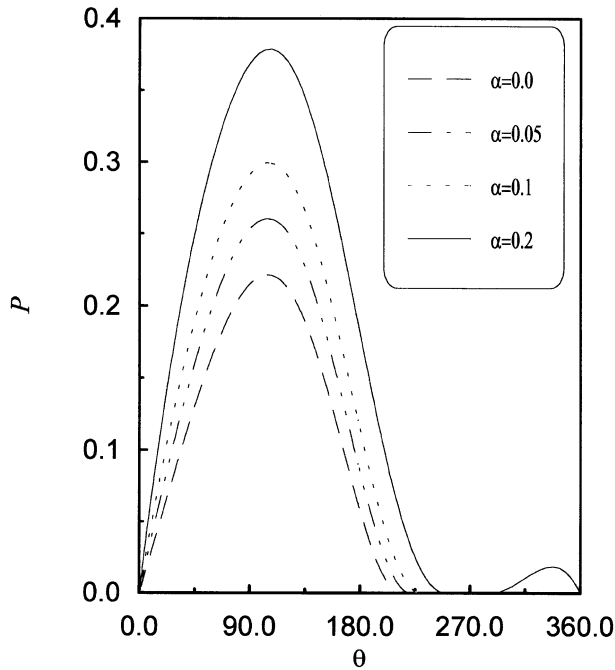
Fig. 5.   Non-dimensional centerline pressure distributions (P) for different α, ε=0.1, ν=1.0 and β=0.75.
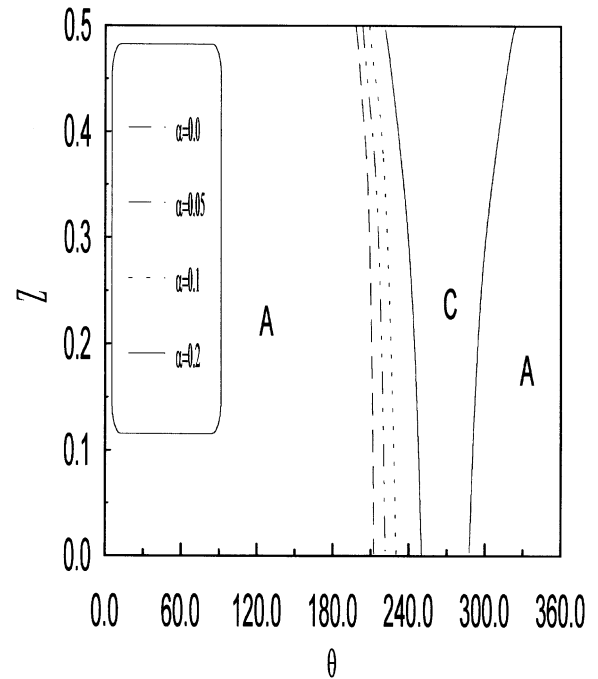

Fig. 6.   Cavitation region boundary shape for different α, ε=0.1 ν=1.0 and β=0.75. (a) denotes active region, and (c) cavitation region.

which causes negative values of the magnetic term [$\alpha H^3(\partial/\partial Z)((H_m(\partial H_m/\partial Z))$] and thus positive magnetic pressures are generated and added to the hydrodynamic pressures resulting from the wedge action ($\partial H/\partial \theta$). The effect of negative magnetic gradient depends mainly on the coefficient (α) such that increases in (α) not only cause increases in the conventional hydrodynamic pressures, but also new regions of positive magnetic pressures are generated. This is shown from the gradual increase in the active region and decrease in the cavitation region. The high magnetic effect at this low eccentricity ratio where the increase in P_{max} from the case of α=0.0 to α=0.2 is about 70%. Fig. 6 obviously indicates the effect of magnetic lubrication on the active and cavitation region boundary shape. There is a clear gradual shrinkage of the cavitation region with increases in α. For α=0.2, a narrow limited region is formed between two active regions: the first is the extended conventional active region (to the left) and the second is the pure magnetic active region (to the right).

Fig. 7 shows the influence of magnetic force coefficient (α) on non-dimensional load capacity for different eccentricity ratio values (ε). As shown, at low eccentricity ratios, there is a considerable increase in the load with increases in α. This improvement of the load is decreased with increases in ε until it becomes negligible at high eccentricity ratios. From a conventional bearing to a magnetic bearing (i.e. α=0.0 to α=0.2) the load carrying capacity increases about 74% at ε=0.1. This value is decreased to 22% at ε=0.3 and becomes 6% at ε=0.6.
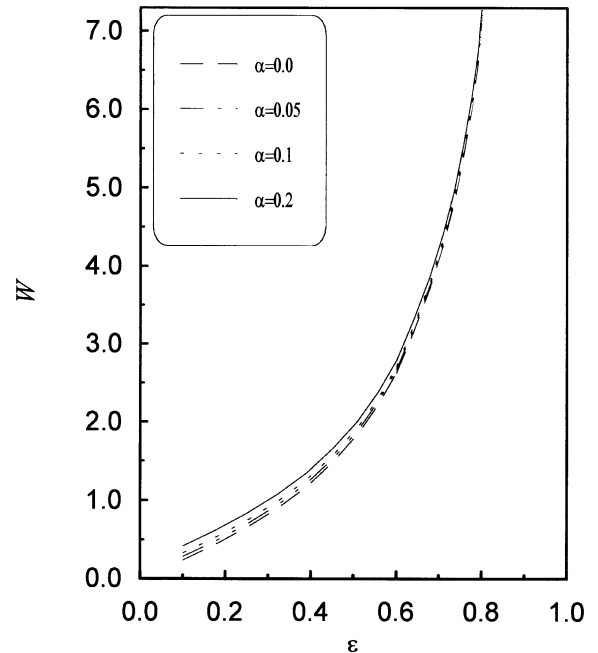

Fig. 7.   Non-dimensional load capacity (W) versus ε and α, ν=1.0 and β=0.75.

Fig. 8 shows the effect of magnetic force coefficient (α) on the journal center attitude angle at different eccentricity ratios. It is clear that there is little decrease in the attitude angle with increases in α at low eccentricity ratio (ε=0.1). At moderate eccentricity ratios, there is a slight increase in attitude angle. Then, there is no significant change at high eccentricity ratios.
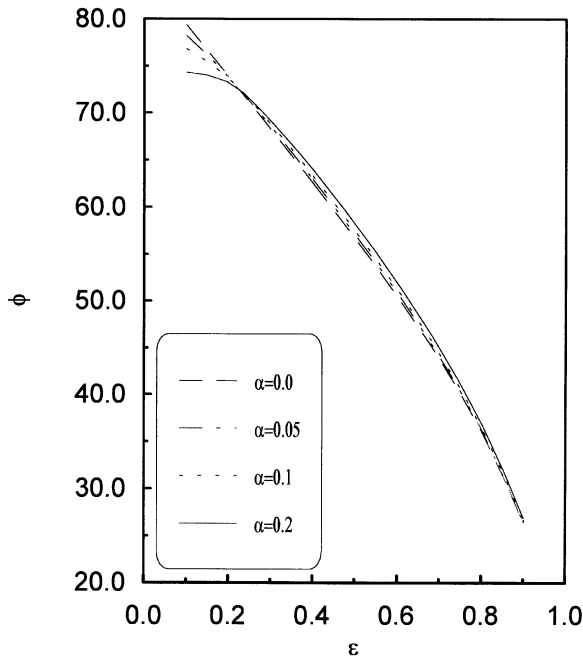
Fig. 8. Attitude angle (Φ) versus ε and α, ν=1.0 and β=0.75.

Fig. 10. Non-dimensional side leakage (Q), for the two bearing configurations versus eccentricity ratio (ε) and magnetic force coefficient (α), ν=1.0 and β=0.75. (a) Unsealed bearing, and (b) sealed bearing.

Fig. 9 shows the effect of magnetic force coefficient (α) on non-dimensional frictional force. As shown, there is no magnetic effect on the friction force. This can be explained as follows: when the eccentricity ratio (ε) is fixed, H (film thickness) is fixed too. The increase in pressure, by the magnetic effect, may not have any significant effect on the pressure gradient ($\partial P/\partial \theta$) and the friction force is nearly constant, see Eq. (15). This means that the magnetic lubrication gives higher load carrying capacity without increases in the friction force and the power losses are not effected. It is also shown that the effect at high eccentricity ratios is negligible.

Fig. 10(a, b) shows the effect of magnetic force coefficient (α) on non-dimensional side leakage for unsealed and sealed bearings, respectively. It is noted clearly from Fig. 10(a) that there is a considerable decrease in the side leakage with increasing coefficient α. Recalling Eq. (17), it is found that the magnetic lubrication has two
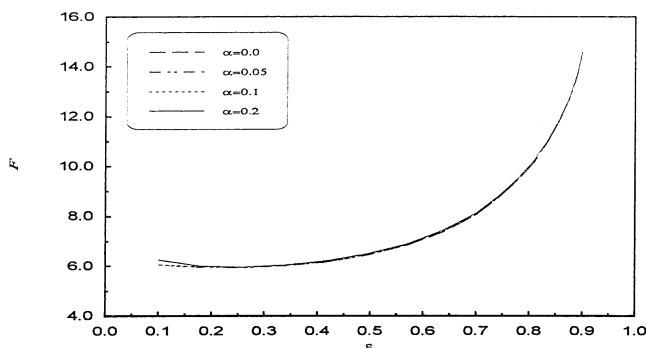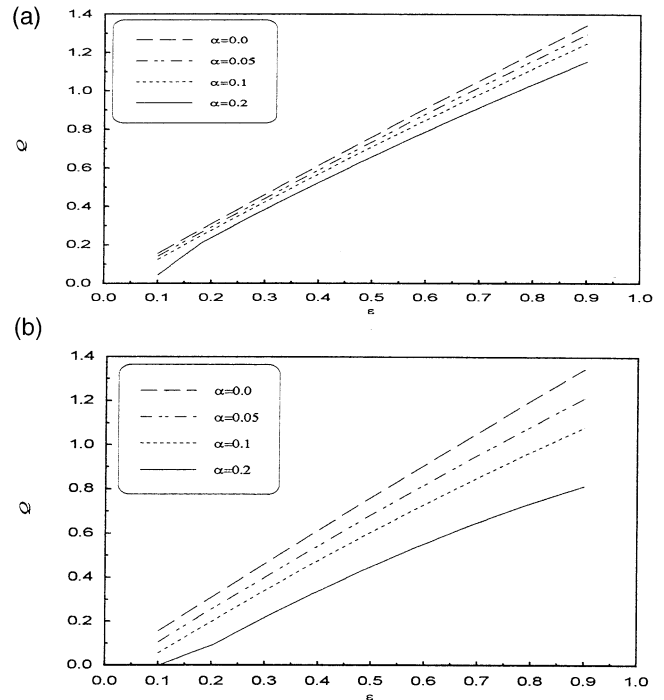
opposite effects: first an increase in pressure and then an increase in pressure gradient ($\partial P/\partial Z$) at the end section. This effect causes an increase in the side leakage. The second effect is the sealing effect by the magnetic force (f_{mz}) at the end section, which causes a decrease in the side leakage. The net effect is the resultant of the above two opposite effects. The results indicate that f_{mz} has the higher effect. For a sealed bearing, Fig. 10(b), there is an additional decrease in the side leakage due to the inward flow from the side oil seals by the axial magnetic force (f_{mz}) through the cavitation region. The decrease may reach such a degree that there is no side leakage for high values of α and low values of ε.

Fig. 11 shows the four stiffness coefficients versus the eccentricity ratio and magnetic force coefficient as a function. It can be seen that the trend of results of the magnetized bearing is nearly the same as the conventional lubricated bearing. The figure shows that the stiffness generally increases as a journal eccentricity increases. This may be explained by the fact that a thinner oil film would inherently deform less than a thicker oil film. Increasing the magnetic force coefficient α causes a slight decrease in the direct vertical stiffness coefficient (K_{xx}) at low and moderate eccentricity ratios, while there is no significant effect on the cross-coupling coefficient K_{xy}. The sign change from negative to positive for the horizontal–vertical cross coupling coefficient (K_{yx}) is significant in the context of system stability and can be seen to occur at an eccentricity ratio of about
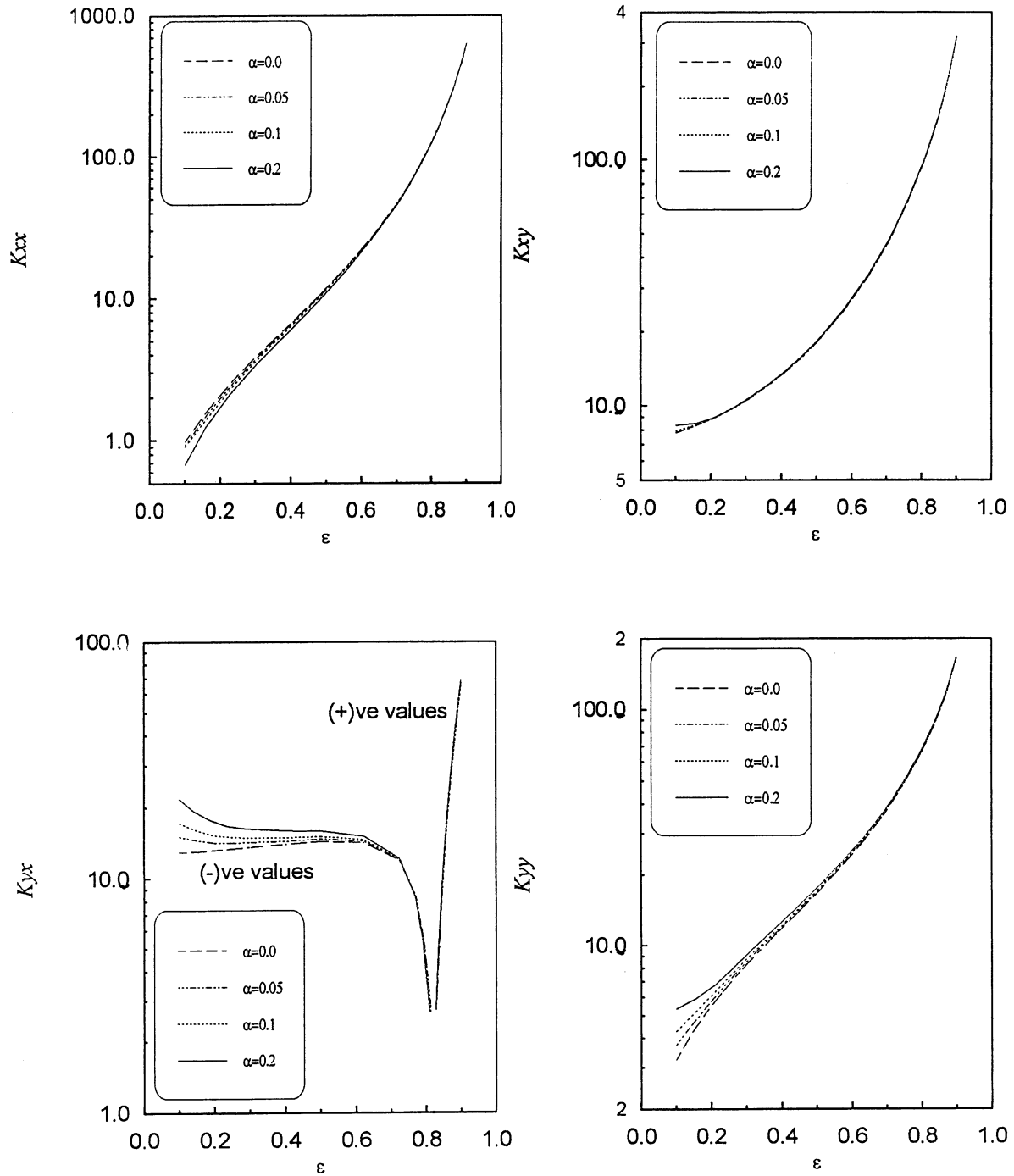

Fig. 9. Non-dimensional friction force (F) versus eccentricity ratio (ε) and magnetic force coefficient (α), ν=1.0 and β=0.75.

Fig. 11.   Stiffness coefficients (K_{ij}) versus ε and α, ν=1.0 and β=0.75.

0.83. The figure clearly shows that there is an increase in the negative values of K_{yx} with increasing α without a change in the sign of the eccentricity ratio. The diagrams for the direct horizontal coefficient (K_{yy}) indicate that the magnetic force coefficient gives rise to the coefficient, especially at low eccentricity ratios. At high eccentricity ratios, the magnetic effect is neglected and no significant change is observed.

Fig. 12 shows variation of the damping coefficients with the eccentricity ratio for different magnetic force coefficient (α) values. Generally speaking, the damping coefficients have high values at large eccentricity ratios with the damping in the load direction C_{xx} by far the principal damping present. At these high eccentricity ratios, the heavy loaded bearings force the journal to operate almost vertically downward resulting in high
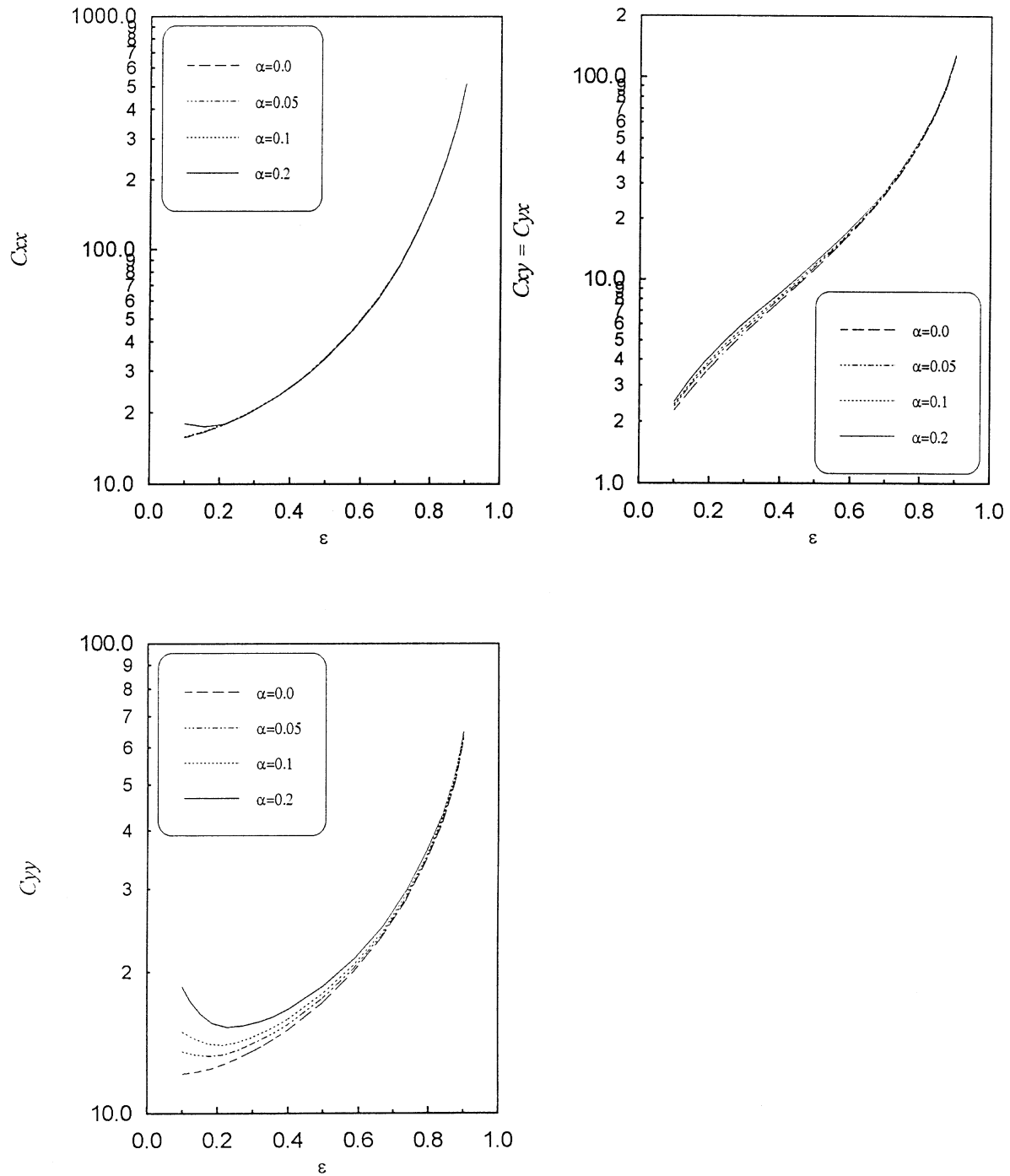
Fig. 12.   Damping coefficients (C_{ij}) versus ε and α, v=1.0 and β=0.75.

vertical stiffness, Fig. 12, and damping but low horizontal properties. It can be seen that the direct damping coefficient C_{xx} is not affected by the magnetic lubrication except at very low eccentricity ratio (ε=0.1) where there is some increase for α=0.2. The cross-coupling damping coefficients C_{xy} and C_{yx}, unlike the corresponding stiffness coefficients, are equal with a little increase in their values due to the increase in the magnetic force coefficient. The direct horizontal damping coefficient (C_{yy})

is greatly affected by the magnetic lubrication where there is a considerable increase with increases in α, especially at low and moderate eccentricity ratios. At high eccentricity ratio, the magnetic effect becomes insignificant and a neglected effect is obtained.

According to the obtained stiffness and damping coefficients, the stability limit of the rigid rotor-bearing system is determined and plotted in Fig. 13. It shows variation of the non-dimensional critical speed with the
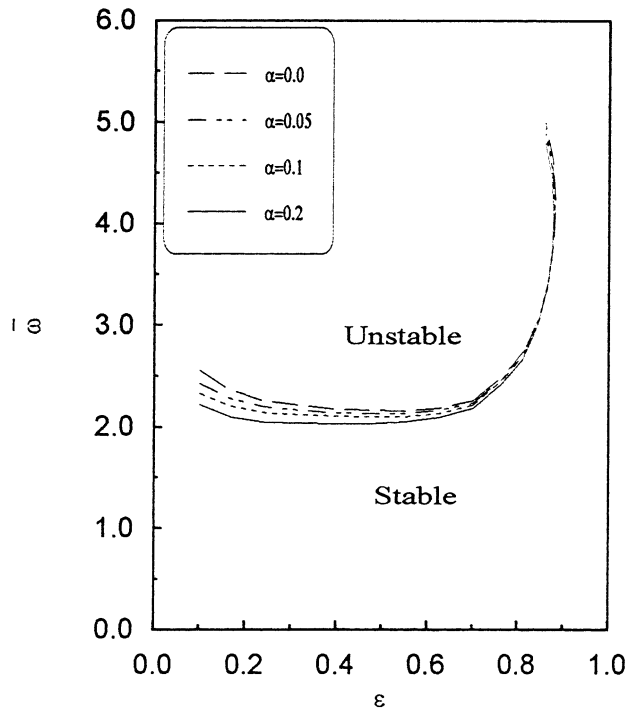
Fig. 13. Non-dimensional critical speed ($\bar{\omega}$) versus ε and α, $\nu=1.0$ and$\beta=0.75$.

eccentricity ratio at different magnetic force coefficients. The rotor is stable for speeds less than the critical value ($\bar{\omega}$) The degree of stability or instability can be indicated by the margin of separation between the journal operating speed and $\bar{\omega}$. It is known that the system instability is associated with the cross-coupling coefficient K_{yx} becoming negative. This is consistent with the obtained inherent stability at an eccentricity ratio where the coefficient K_{yx} is positive. The figure shows a slight destabilizing effect with the increase in magnetic force coefficient, especially at low and moderate eccentricity ratios. At high eccentricity ratio the hydrodynamic effect is the major effect and the magnetic effect is neglected. The point at which the system is always stable does not change.

8. Conclusions

1. The bearing performance is significantly modified when the magnetic effects are comparable with the hydrodynamic effects, namely, when the bearing operates at low eccentricity ratios, the magnetic field is high, the rotation speed is low and the relative clearance is large. Far from such conditions the hydrodynamic effects prevail considerably and an insignificant effect for the magnetic lubrication is obtained.
2. Improving the bearing performance characteristics can be greatly increased not only by proper selection of the magnetic field model, but also with careful

choice of the design parameters of the model used. The axial parabolic model shows maximum sealing effect if $\beta=0.5$.
3. The analysis reveals that the magnetic force is able to increase the bearing load if a proper magnetic field distribution model is used. Negative gradients of the applied are necessary. This increase is due to the increased pressure and decreased cavitation region; the extent of the load-carrying (active) region becomes larger.
4. The side leakage is highly decreased. It can be completely eliminated by appropriately designing the bearing geometry and the magnetic field.
5. Little change of the attitude angle is obtained.
6. The magnetic lubrication has negligible effect on the frictional force.
7. The dynamic characteristics of the magnetized bearing are modified such that a destabilizing effect of the rotor-bearing system is obtained. The axial parabolic model shows a slight decrease in the rotor critical speed.

References

[1] Saynatjoki M, Holmberg K. Magnetic fluids in sealing and lubrication — a state of art review, vol. 10. Technical Research Center of Finland, Feb 1982, p. 119–31.
[2] Rosensweig RE, Kaiser R, Miskolczy G. Viscosity of magnetic fluid in a magnetic field. J Colloid Interface Sci 1969;29(4):680–6.
[3] Rosensweig RE. Magnetic fluids. Sci Am 1982;247(4):124–32.
[4] Miyake S, Takahashi S. Sliding bearing lubricated with ferromagnetic fluid. ASLE 1985;28:461–6.
[5] Goldowsky M. New methods for sealing, filtering, and lubricating with magnetic fluids. IEEE Trans Magnetics 1980;16:382–6.
[6] Moskowitz R, Ezekiel FD. Magnetic fluids — something to consider. Instruments Control Syst 1975;48:41–5.
[7] Williams RA, Malsky H. Some experiences using a ferrofluid seals against a liquid. IEEE Trans Magnetics 1980;16:379–81.
[8] Bonvouloir J. Experimental study of high speed sealing capability of single stage ferrofluidic seals. ASME J Tribol 1997;119:416–21.
[9] Gorla JSR, Ramalingam K, Adluri I. Magnetohydrodynamic breaking. ASME J Tribol 1995;117:724–8.
[10] Broge JL. Valveless damping suspension system, Tech briefs. J Automotive Eng Int 1999;December:50–2.
[11] Tipei N. Theory of lubrication with ferrofluids: application to short bearings. ASME J Lubrication Technol 1982;104:510–5.
[12] Tipei N. Overall characteristics of bearings lubricated with ferrofluids. ASME J Lubrication Technol 1983;105:466–75.
[13] Tarapov IE. Movement of a magnetizable fluid in the lubricating layer of a cylindrical Bearing. Magnetohydrodynamics 1972;8:444–8.
[14] Sorge F. A numerical approach to finite journal bearings lubricated with ferrofluid. ASME J Tribol 1987;109:77–82.
[15] Zhang Y. Static characteristics of magnetized journal bearing lubricated with ferrofluid. ASME J Tribol 1991;113:533–8.
[16] Zelazo RE, Melcher JR. Dynamic and stability of ferrofluids: surface interaction. J Fluid Mech 1969;39:1–24.
[17] Chang HS, Chi CQ, Zhao PZ. A theoretical and experimental

study of ferrofluid lubricated four-pocket journal bearings. J Magn Magn Mater 1987;65:372–4.

[18] Cowley MD, Rosensweig RE. The interfacial stability of ferro- magnetic fluid. J Fluid Mech 1967;30:671–88.

[19] Lund JW. Review of the concept of dynamic coefficients for fluid film journal bearings. ASME J Tribol 1987;109:37–41.